

MIS SLOW-WAVE STRUCTURES OVER A WIDE RANGE OF PARAMETERS

James P. K. Gilb and Constantine A. Balanis

Department of Electrical Engineering, Telecommunications Research Center
Arizona State University, Tempe, Arizona 85287-7206

ABSTRACT

The high dielectric losses of the semiconducting substrates used in MMIC's and VLSI interconnects can strongly affect all of the characteristics of these lines. Since no single approximate formulation is accurate over a wide range of substrate parameters or over a large frequency range required for a transient analysis, a full-wave approach is required to analyze these structures. Multi-conductor MIS structures are analyzed with the spectral domain approach over a wide range of frequency and substrate loss. The modal attenuation and propagation constants are presented two and four conductor structures as a function of the substrate loss tangent. Single conductor structures are characterized with contour plots showing the complex effective dielectric constant as a function of both frequency and conductivity.

INTRODUCTION

Planar MIS structures are important components in the design of MMIC's and high-speed digital integrated circuits. The wide range of semiconductor resistivities used for these structures and wide bandwidth of the pulses requires the use of full-wave techniques to accurately analyze these structures. Initial research of these structure used a parallel plate waveguide approximation to determine the complex propagation constant [1], [2] which gives good results only for very wide center conductors. Mode-matching has also been applied to give accurate results for a limited range of substrate parameters [3], [4]. The Spectral-Domain Approach (SDA) has also been used to characterize these types of structures for Coplanar Waveguide (CPW) [3], for single and coupled microstrips on a single substrate [5], [6], and for multiple microstrips on multi-layer, lossy substrates [7].

Although planar MIS structures have received some attention, these studies have only covered a few special cases over a limited range of frequency and substrate loss. In addition, multi-conductor structures, such as those found in high-speed, high-density digital interconnects, have received very little attention. This paper studies lossy multi-layer,

multi-conductor microstrip structures using the SDA. The modal attenuation and propagation constants of these structures are given over an extremely wide range of substrate parameters and frequencies, covering all three regions; low loss, slow wave, and skin effect.

THEORY

The SDA has been discussed extensively in previous works and so the technical details are omitted here. A very good explanation of the method can be found in [8] and an excellent list of references are given in [9]. The Green's function for structures with multiple substrates and/or superstrates can be computed using a simple recursive formulation given in [10]. The geometry for multi-layer, multi-conductor interconnects is shown in Fig. 1. Two substrates are shown in the figure, although any finite number of substrates can be easily considered using the recurrence formulation from [10].

For a conductor centered at $x = x_i$ with a width $w = w_i$, the current density expansion functions used in this paper are given by:

$$J_{z_n}^i(x) = a_n^i(j)^n \frac{T_n(X_i)}{\sqrt{1 - (X_i)^2}} \quad (1)$$

$$J_{x_n}^i(x) = -jb_n^i(j)^n \frac{w_i}{2} U_{n-1}(X_i) \sqrt{1 - (X_i)^2} \quad (2)$$

for $n = 0, 1, 2, \dots$, $X_i = 2(x - x_i)/w_i$ and $|x - x_i| \leq w_i/2$. $T_n(x)$ and $U_n(x)$ are the Chebyshev polynomials of the first and second kind, respectively, as given in [11]. Results obtained with this method have been compared and agree very closely with results presented in the literature [7], [6]. Throughout this investigation, ϵ_{eff}^* refers to the complex effective relative dielectric constant with real part ϵ'_{eff} and imaginary part ϵ''_{eff} ($\epsilon_{\text{eff}}^* = \epsilon'_{\text{eff}} - j\epsilon''_{\text{eff}}$).

For a "good" dielectric, it is usually assumed that the loss tangent is constant with frequency. For semiconductors or conductors, on the other hand, it is usually assumed that the conductivity or resistivity is constant with frequency. Since accurate measurements of the complex dielectric constant versus frequency are not readily available for most materials, one of the two assumptions, either constant $\tan \delta$

IF2

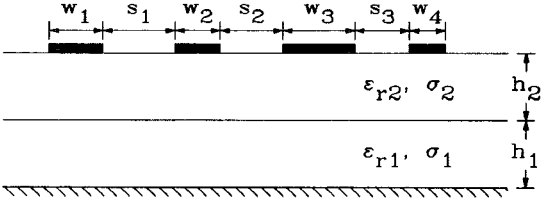


Figure 1: Geometry of an asymmetric two-substrate, multi-conductor interconnect.

or constant σ , will be used in this paper. In either case, it will be made clear which assumption is used.

RESULTS

To study the characteristics of MIS slow-wave structures, a two-substrate, coupled microstrip structure is used where the upper substrate is lossless or has very low-loss ($\tan \delta_2 \ll 1$) and the lower substrate is characterized by either a loss tangent or conductivity. The behavior of this structure as a function of frequency and dielectric loss can be divided up into three main regions: 1) low-loss region, 2) slow-wave region, and 3) skin-effect region. Fig. 2 shows ϵ'_{eff} and α_d for single (isolated) and coupled (even and odd modes) microstrips on two substrates as a function of the loss tangent of the lowest substrate computed using the lossy SDA approach. Since the frequency is held constant at 1 GHz, varying the loss tangent is equivalent to varying the conductivity (for this configuration, $\sigma(\Omega^{-1}m^{-1}) = 0.540 \tan \delta_1$). For $\tan \delta_1 \ll 1$, the structure is in the low-loss region and the losses do not have a noticeable effect on ϵ'_{eff} . On the other hand, α_d increases linearly with increasing $\tan \delta_1$, as is the normal case for low-loss structures. In this region, the lower substrate has the characteristics of a “good” dielectric.

When $\tan \delta_1$ is very large, then the structure is said to be operating in the skin-effect region. With increasing frequency or dielectric loss, the dielectric loss tends to decrease as more of the fields are contained in the lossless, upper substrate rather than in the lossy, lower substrate. In Fig. 2, α_d decreases with a slope of $-1/2$ on the log-log scale, indicating a $1/\sqrt{\tan \delta_1}$ behavior, consistent with the behavior of the conductor loss coefficient due to the skin effect which has a $1/\sqrt{\sigma_1}$ behavior. ϵ'_{eff} is relatively constant, decreasing slightly with increasing $\tan \delta_1$. In this region, the lower substrate has the characteristics of a “good” conductor.

For moderate $\tan \delta_1$ the structure is in the slow-wave region, where the slow-wave factor, $\lambda_0/\lambda = \sqrt{\epsilon'_{\text{eff}}}$, increases due to the increase in ϵ'_{eff} . Unlike the lossless microstrip case, ϵ'_{eff} in the slow wave region is much larger than the relative dielectric constants of either of the substrate layers. The upper limit of ϵ'_{eff} , which is achieved for very wide center conductors, is given by the static value of the Maxwell-Wagner permittivity [12], $\epsilon'_{rs} = \epsilon_{r2}(h_1 + h_2)/h_2$. In the slow-wave region, the dielectric loss coefficient, α_d , decreases linearly with increasing $\tan \delta_1$, reaches a minimum

point, and then begins to increase linearly again. The minimum point can be predicted using the parallel plate waveguide approximation [2] and occurs for a conductivity of

$$\sigma_{\min} = \sqrt{\frac{3\epsilon_0\epsilon_{r2}}{\mu_0\mu_{r2}h_1h_2}} \quad (3)$$

or for a loss tangent of

$$\tan \delta_{\min} = \frac{c}{\omega\epsilon_{r1}} \sqrt{\frac{3\epsilon_{r2}}{\mu_{r2}h_1h_2}}. \quad (4)$$

For this structure, the above equation predicts minimum attenuation for $\tan \delta_{\min} = 102$, which is close to the location of the actual minimum.

Connecting the low-loss and slow-wave regions and slow-wave and skin-effect regions are the transition regions. These regions are characterized by maximum ϵ''_{eff} and hence maximum α_d . Also in these regions, ϵ'_{eff} is changing rapidly from either the low-loss to the slow-wave values or from the slow-wave to the skin-effect values. For all regions the even mode ϵ'_{eff} and ϵ''_{eff} are higher than those of the odd mode since the fields of the even mode are concentrated more in the lower, lossy substrate. The odd mode, on the other hand, has most of its fields concentrated in the air and in the lossless, upper substrate. Thus, the odd mode is attenuated less and changes in the dielectric loss do not affect the odd mode ϵ'_{eff} as much as they do that of the even mode.

A four line, symmetric microstrip structure on an Si-SiO₂ substrate is analyzed in Fig. 3 and Fig. 4 as a function of the conductivity of the Si layer at a frequency of 1 GHz. The structures analyzed in Figs. 3- all have a layer of SiO₂ ($\epsilon_r = 4$) on top of a layer of Si ($\epsilon_r = 12$). ϵ'_{eff} for each of the four independent modes is given in Fig. 3 with the corresponding α_d 's presented in Fig. 4. The plus and minus signs next to the mode numbers refer to the relative magnitudes of the currents on each of the conductors for that mode [13]. The attenuation coefficients of each of the four modes reach a minimum in the slow-wave region for conductivities between 60 and 200 $\Omega^{-1}m^{-1}$. The predicted minimum for a single strip on this substrate using (3) is 194 $\Omega^{-1}m^{-1}$. The slowest mode, mode 3, has even/even symmetry which concentrates most of the fields in the substrates. Thus the ϵ'_{eff} for this mode is affected the most by changes in the conductivity of the Si layer and has higher losses. The fastest mode, mode 2, however, has odd/odd symmetry and so the electric fields for this mode are concentrated more in the air and upper substrate and so it has lower losses and is affected less by changes in the conductivity of the Si layer.

To illustrate how frequency and dielectric losses affect the complex ϵ_{eff} , contour plots of ϵ'_{eff} and $\log_{10}(\epsilon''_{\text{eff}})$ are presented in Figs. 5 and assuming that the conductivity is constant with frequency. In Fig. 5, the large open space in the lower, center part of the contour plot is the slow-wave region. In this area, ϵ'_{eff} is a maximum and changes very little with either frequency or dielectric loss, maintaining a value of around 28. The low-loss region is located in the upper left of Fig. 5. In Fig. 5, ϵ'_{eff} decreases rapidly from

its slow-wave value, approaching the low-loss, quasi-static value. It then begins to increase with increasing frequency, due to the dispersive properties of microstrip.

The skin effect region is in the upper right of the contour plot. The transition for the slow-wave value of ϵ'_{eff} to its skin-effect value is fairly rapid. The value of ϵ'_{eff} in the skin-effect region is lower than that of the low-loss region because the low-loss region is a two-substrate structure dominated by the Si layer ($\epsilon_r = 12$) while in the skin-effect region it is essentially a one-substrate structure of SiO_2 ($\epsilon_r = 4.0$).

The slow-wave, low-loss, and skin-effect regions in Fig. 5 are located in the same areas as in Fig. 5. One difference in the behavior of the real and complex parts of ϵ_{eff} is that within each of the three regions, the value of ϵ'_{eff} is relatively constant with changing frequency and dielectric loss, while the value of ϵ''_{eff} is always changing within the regions. Another point to note is that when ϵ'_{eff} is a maximum (in the center of the slow-wave region), ϵ''_{eff} , and hence the dielectric losses, are at a minimum. Using (3), the value of σ which gives minimum dielectric loss is $\sigma_{\min} = 0.092(\Omega\text{mm})^{-1}$, which is close to actual value for this structure.

CONCLUSION

The presence of high dielectric losses or a conductivity that is constant with frequency requires the use of a full-wave analysis. The SDA was used to accurately analyze multi-layer, multi-conductor structures over a wide range of frequency and substrate loss. Results for single, two, and four conductor structures were presented which show how the substrate dielectric loss affects both the real and imaginary parts of the effective dielectric constant. MIS slow-wave structures were analyzed using for a single conductor on an Si- SiO_2 substrate. Contour plots of the complex effective dielectric constant showed the locations and characteristics of three regions of operation, slow-wave, low-loss, and skin-effect.

REFERENCES

- [1] H. Guckel, P. A. Brennan, and I. Palócz, "A parallel-plate waveguide approach to microminiaturized, planar transmission lines for integrated circuits," *IEEE Trans. Microwave Theory Tech.*, vol. MTT-15, pp. 468-476, Aug. 1967.
- [2] H. Hasegawa, M. Furukawa, and H. Yanai, "Properties of microstrip line on Si- SiO_2 system," *IEEE Trans. Microwave Theory Tech.*, vol. MTT-19, pp. 869-881, Nov. 1971.
- [3] Y. Fukuoka, Y.-C. Shih, and T. Itoh, "Analysis of slow-wave coplanar waveguide for monolithic integrated circuits," *IEEE Trans. Microwave Theory Tech.*, vol. MTT-31, pp. 567-573, July 1983.
- [4] C.-K. C. Tzuang and T. Itoh, "High-speed pulse transmission along a slow-wave CPW for monolithic microwave integrated circuits," *IEEE Trans. Microwave Theory Tech.*, vol. MTT-35, pp. 697-704, Aug. 1987.
- [5] J. P. K. Gilb and C. A. Balanis, "Transient analysis of distortion and coupling in lossy coupled microstrips," *IEEE Trans. Microwave Theory Tech.*, vol. MTT-38, pp. 1894-1899, Dec. 1990.
- [6] D. Mirshekari-Syahkal, "An accurate determination of dielectric loss effect in monolithic microwave integrated circuits including microstrip and coupled microstrip lines," *IEEE Trans. Microwave Theory Tech.*, vol. MTT-31, pp. 950-954, Nov. 1983.
- [7] T.-C. Mu, H. Ogawa, and T. Itoh, "Characteristics of multiconductor, asymmetric, slow-wave microstrip transmission lines," *IEEE Trans. Microwave Theory Tech.*, vol. MTT-34, pp. 1471-1477, Dec. 1986.
- [8] T. Uwano and T. Itoh, "Spectral domain approach," in *Numerical Techniques for Microwave and Millimeter-Wave Passive Structures* (T. Itoh, ed.), ch. 5, pp. 334-380, New York: John Wiley and Sons, 1989.
- [9] R. H. Jansen, "The spectral-domain approach for microwave integrated circuits," *IEEE Trans. Microwave Theory Tech.*, vol. MTT-33, pp. 1043-1056, Jan. 1985.
- [10] J. P. Gilb and C. A. Balanis, "Pulse distortion on multilayer coupled microstrip lines," *IEEE Trans. Microwave Theory Tech.*, vol. MTT-37, pp. 1620-1628, Oct. 1989.
- [11] M. Abramowitz and I. A. Stegun, *Handbook of Mathematical Functions*. New York: Dover Publications, Inc., 1972.
- [12] A. R. Von Hippel, *Dielectrics and Waves*. New York: John Wiley and Sons, Inc., 1954.
- [13] J. P. K. Gilb and C. A. Balanis, "Asymmetric, multiconductor, low-coupling structures for high-speed, high-density digital interconnects," *IEEE Trans. Microwave Theory Tech.*, vol. MTT-39, pp. 2100-2106, Dec. 1991.

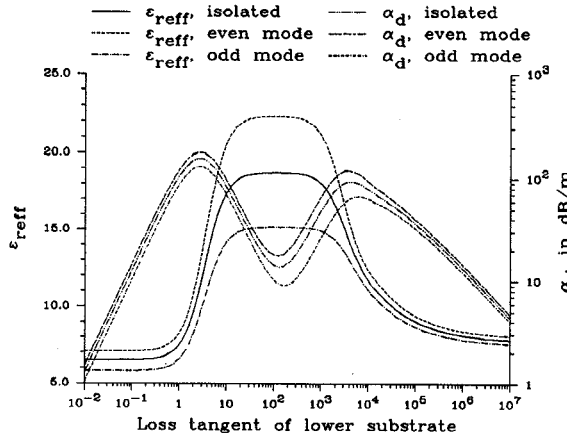


Figure 2: ϵ'_{eff} and α_d for single and coupled microstrips as a function of the loss tangent of the lower substrate at a frequency of 1 GHz ($\epsilon_{r1} = \epsilon_{r2} = 9.7$, $\tan \delta_2 = 0$, $h_1 = 0.5\text{mm}$, $h_2 = 0.135\text{mm}$, $w = 0.6\text{mm}$, $s = 0.6\text{mm}$).

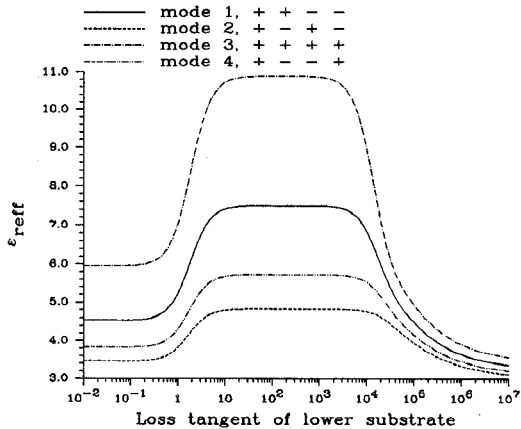


Figure 3: ϵ'_{eff} for symmetric four-line interconnect as a function of the loss tangent of the lower substrate at a frequency of 1 GHz ($\epsilon_{r1} = 12$, $\epsilon_{r2} = 4$, $\tan \delta_2 = 0$, $h_1 = 0.2\text{mm}$, $h_2 = 0.05\text{mm}$, $w = 0.16\text{mm}$, $s = 0.16\text{mm}$).

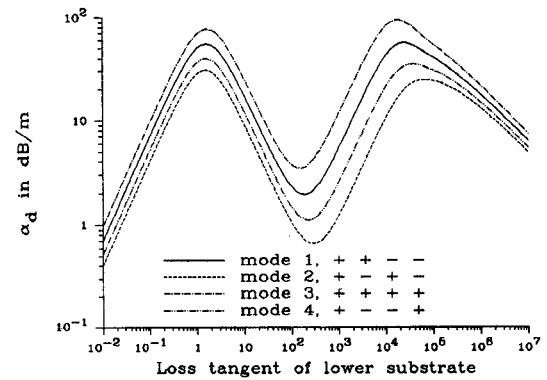


Figure 4: α_d for symmetric four-line interconnect as a function of the loss tangent of the lower substrate at a frequency of 1 GHz ($\epsilon_{r1} = 12$, $\epsilon_{r2} = 4$, $\tan \delta_2 = 0$, $h_1 = 0.2\text{mm}$, $h_2 = 0.05\text{mm}$, $w = 0.16\text{mm}$, $s = 0.16\text{mm}$).

